Applied Physics Letters

Coupled very-high permittivity dielectric resonators for clinical MRI

Cite as: Appl. Phys. Lett. **117**, 103701 (2020); https://doi.org/10.1063/5.0016086
Submitted: 01 June 2020 . Accepted: 25 August 2020 . Published Online: 09 September 2020

Viacheslav Ivanov, Alena Shchelokova, Anna Andreychenko, and Alexey Slobozhanyuk

Applied Physics Letters ARTICLE scitation.org/journal/apl

Coupled very-high permittivity dielectric resonators for clinical MRI

Cite as: Appl. Phys. Lett. **117**, 103701 (2020); doi: 10.1063/5.0016086
Submitted: 1 June 2020 · Accepted: 25 August 2020 ·
Published Online: 9 September 2020

Viacheslav Ivanov,[1] Alena Shchelokova,[1] Anna Andreychenko,[1,2] and Alexey Slobozhanyuk[1,a)]

AFFILIATIONS

[1]Department of Physics and Engineering, ITMO University, St. Petersburg 197101, Russia
[2]Research and Practical Clinical Center for Diagnostics and Telemedicine Technologies of the Moscow Health Care Department, Moscow 109029, Russia

[a)]Author to whom correspondence should be addressed: a.slobozhanyuk@metalab.ifmo.ru

ABSTRACT

Dielectric resonators made of high permittivity materials with low losses have been extensively studied for application in magnetic resonance imaging (MRI) and magnetic resonance spectroscopy. They can focus, redistribute, and enhance the radio frequency magnetic field in a controlled way. In this Letter, we investigate coupled very-high permittivity dielectric resonators for clinical bilateral breast MRI. The resonators are tuned to support a TE mode within the frequency of 3 T MRI and implemented as a pair of coaxial hollow cylinders consisting of ceramic rings with extremely high permittivity ($\varepsilon \sim 870$) and low loss. We study the electromagnetic coupling between two resonators placed in the near field and analyze the impact of symmetric and antisymmetric mode excitation on the sensitivity of the MRI machine. We experimentally verify that the coupling of the mode with symmetric field distribution to the radio frequency body birdcage coil allows us to enhance the receive sensitivity substantially and to decrease the excitation power needed to provide the optimal transmit efficiency, thus making the MRI procedure safer. Our work offers a practical method to realize a simple yet very effective system based on dielectric resonators for bilateral breast imaging.

Dielectric resonators are designed to replace resonant cavities without the need for lumped elements such as inductors and capacitors.[1] These resonators usually have a higher quality factor, more compact dimensions, temperature stability, and a low cost in comparison with their metallic counterparts. A large number of different electromagnetic modes can be excited in dielectric structures depending on both the geometry and the number of resonators.[2]

A majority of dielectric resonators were designed to operate in microwave and millimeter frequency ranges.[3] However, the abilities of such structures to manipulate and sculpt near electromagnetic field leads to beneficial applications in the radio frequency range, including applications in magnetic resonance imaging (MRI) and magnetic resonance spectroscopy (MRS).[4] Dielectric resonators can be employed as an alternative to conventional radiofrequency coils.[5] They are easier in fabrication than traditional radiofrequency coils, and it is possible to tune such resonance systems to the desired frequency, just optimizing its geometry without additional circuits and lumped elements. Various configurations of resonators and dielectric materials were proposed providing different benefits: significant local enhancement of the signal-to-noise ratio (SNR),[6] the possibility to achieve a more homogeneous radio frequency magnetic field within the sample,[7] and to reduce electromagnetic coupling between the elements of receive arrays.[8]

Several devices based on dielectric resonators were designed to operate at ultrahigh static magnetic field strengths (frequency range above 298 MHz), for example, an annular dielectric resonator made from distilled water to operate at 7 T,[9] its later segmented design facilitated with metallic connectors,[10] transceive arrays based on dielectric resonator antennas,[8] and detunable receive arrays at 7 T.[11] Also, similar structures found their applications in magnetic resonance (MR) microimaging, for example, ceramic resonators, which were proposed for 14.1 T[12,13] and 17 T.[14] However, for field strengths below 7 T, i.e., 1.5–3 T, conventional dielectric resonator dimensions become very large, due to the increase in the wavelength, making it impossible to use them in clinical MRI. In some particular cases, it is possible to apply the idea of artificial dielectrics to reduce the dimensions,[15] but such resonators are still too large for widespread use. Therefore, to make use of dielectric resonators at clinical field strength, they should be realized by employing materials with very high dielectric permittivity and low losses.[16–18]

Recently, a targeted MRI concept based on the implementation of a unique ceramic material resonator of permittivity 1000 was proposed for unilateral breast imaging.[19] However, unilateral imaging (scanning only of one breast) is usually performed when the patient has had a breast removed. In a typical screening case, bilateral imaging is more convenient for both patients and clinicians since no additional time is needed to lie inside the MRI machine and to reinstall the equipment. As a result, patient comfort and satisfaction are increased, as well as the throughput of MRI cabinets. Also, bilateral breast imaging has additional benefits vs unilateral for patients who were already diagnosed with breast cancer if they have lesions that are known to affect both breasts at a higher rate.[20]

In this Letter, we investigate the possibility to control the spatial distribution of the electromagnetic field within the bore of the clinical 3 T MRI machine with dielectric resonators with potential application for bilateral breast imaging. For this purpose, we design structure as a pair of coaxial hollow cylinders composed of Mg-doped $BaSrTiO_3$ ceramic[18] rings with extremely high permittivity ($\varepsilon \sim 870$) and low loss ($\tan\delta \sim 12 \times 10^{-4}$ at 123 MHz). We analyze the electromagnetic coupling between two resonators placed in the near field and study the impact of symmetric and antisymmetric mode excitation on the sensitivity of the MRI machine. Since the proposed device is wireless, i.e., it does not require a radiofrequency cable connection within the scanner, it can be applied to the MRI machine of any vendor. We demonstrate an application of such a system to the bilateral breast imaging using realistic phantoms and experimentally show that the coupling of the mode with symmetric field distribution to the radiofrequency body coil allows enhancement of the transmit efficiency and receive sensitivity of the latter.

The system under study is formed as a pair of equally oriented hollow cylindrical resonators (Fig. 1) and oriented inside the body birdcage coil as required for bilateral breast MRI. The proposed system' operation is based on the targeted MRI concept,[19] i.e., on the local redistribution and passive focusing of the radiofrequency magnetic field of the body birdcage coil through electromagnetic coupling with dielectric resonators surrounding the target area. By optimizing the height and diameter of both dielectric resonators, the $TE_{01\delta}$ mode was tuned to the Larmor frequency of the 3 T MRI machine (123 MHz). In the considered here resonators configuration, their main axes of symmetry are orthogonal to the static magnetic field. In such a configuration, the radiofrequency magnetic field produced by the body birdcage coil (namely, B_1^+ field—right circularly polarized component of the radiofrequency magnetic field B_1) can excite $TE_{01\delta}$ mode of the resonator.[21] This mode is characterized by the magnetic field localized in the cavity of the resonator (i.e., in the region of interest) and the electric one concentrated inside high permittivity dielectric material (i.e., on the outer side). While the case of excitation of a single dielectric resonator within the MRI bore has been well-studied previously,[19,21] the placement of the second one changes the situation completely. A giant coupling between two resonators occurs, and therefore, the original resonance frequency splits into two, which corresponds to the excitation of symmetric and antisymmetric modes.

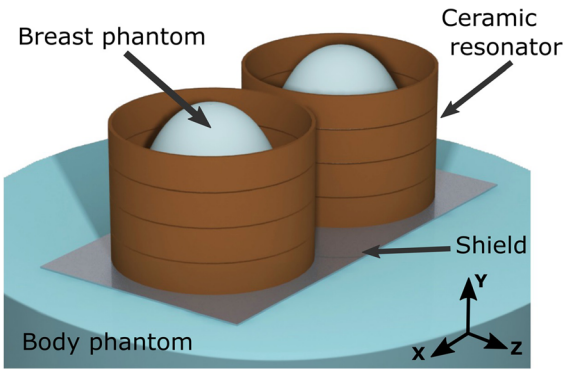

FIG. 1. Schematic view of the proposed setup: coupled dielectric resonators ($\varepsilon \sim 870$ and $\tan\delta \sim 12 \times 10^{-4}$ measured at 123 MHz) with the metallic shield and breast ($\varepsilon = 48.6$, $\sigma = 0.57$ S/m) and body ($\varepsilon = 38$, $\sigma = 0.3$ S/m) phantoms. A thin rectangle metallic shield was used to preserve the efficiency of the dielectric resonator in proximity to the body.

First, we studied the dependence of resonator coupling on the distance between them. Figure 2(a) shows the simulated system of two resonators loaded with big phantom imitating the human body (with dimensions 780 mm in X, 460 mm in Z, and 113 mm in Y directions) and two small phantoms mimicking medium-size breasts (with a base diameter of 91 mm and a height of 102 mm). Big phantom had a relative dielectric permittivity of 38 and a conductivity of 0.3 S/m. The material parameters of the small phantoms were $\varepsilon = 48.6$ and $\sigma = 0.57$ S/m; these values were obtained from the parameters for fat and glandular tissues forming the breast under the assumption that the fat and glandular tissue averaged volume ratio is 3:1.[22] The numerical simulations were performed using CST Microwave Studio 2019. A non-resonant loop was placed precisely in the center above one of the resonators to excite the $TE_{01\delta}$ mode. The distance d between the centers of the resonators was changed from 30 to 16 cm. To minimize electromagnetic coupling between dielectric resonators and big phantom, metallic disks were placed between them. The diameter of each metallic disk was 19 cm. It is worth noting that metallic disks were united, forming a figure-eight plate when the distance between the centers of the resonators was smaller than 19 cm.

Figure 2(b) shows the numerically calculated spectral dependencies of the reflection coefficient (S_{11}) of the non-resonant loop for different distances between the resonators. For $d = 30$ cm between the centers, the coupling between the two resonators was small, and only one resonance has been observed. Upon gradually decreasing the distance d, the coupling between the resonators was increased. For $d = 20$ cm, we have observed the clear splitting of the original resonance. The smaller the distance d, the stronger splitting of the resonances occurred. With a further distance decrease, two minima of the curve were more clearly distinguished. The frequency gap between them increased from 4.1 MHz for $d = 20$ cm to 10.6 MHz for $d = 16$ cm. The two minima in the reflection coefficient correspond to the excitation of symmetric and antisymmetric modes [see the magnetic field maps in the insets in Fig. 2(b)].

To imitate MRI conditions, we performed a numerical simulation with the realistic body birdcage coil model (high-pass, 16 legs, 70 cm in diameter, and 49 cm in length). The first mode of the birdcage coil was preliminarily tuned and matched at 123 MHz with the phantoms only (without dielectric resonators). Then, the resonators were placed along the y-coordinate perpendicular to the main static magnetic field in the center of the birdcage coil with the same set of phantoms [Fig. 3(a)]. Due to the physical restrictions (i.e., the distance between

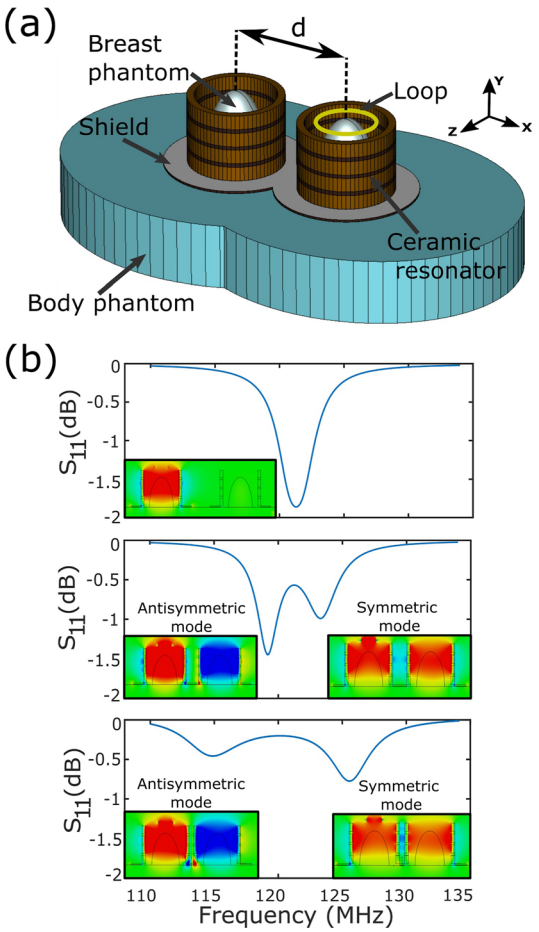

FIG. 2. (a) Setup of the numerical model: two coupled resonators with a loop coil placed above one of them. Distance (d) between the centers of the resonators was varied to obtain different coupling (b). Reflection coefficient (S_{11}) of the loop coil for $d = 30$, 20, and 16 cm top-down, respectively. The insets demonstrate magnetic field distributions (real part of the Hy component) in the central cross section (XY plane) for low-frequency (antisymmetric) and high-frequency (symmetric) modes, respectively. Color bars were normalized to min-max values for each case, respectively.

breasts), we chose a distance of 16 cm between the centers of the dielectric resonators. We simulated two setups: the first one corresponds to the tuning of the resonators' antisymmetric mode to 123 MHz and the second one—to the adjustment of the symmetric mode to 123 MHz. To perform such tuning, we placed three 13-mm-thick spacers with a dielectric permittivity of 3.5 between very-high permittivity dielectric rings in the first case and three 2-mm-thick spacers in the second one. A figure-eight shielding plate is used in numerical simulations and simplified to a rectangle plate with two round holes, performing the same effect.

Since the body birdcage coil is also a large resonator with a particular near field profile at the operational MR frequency, the placement of an additional resonant system (pair of dielectric resonators) led to the excitation of certain modes with different coupling strength (we have also studied an excitation of these modes with a combination of several plane waves - see supplementary material for details). We analyzed the spectral dependences of the magnetic field amplitude within the region of the breast and found two maxima corresponding to low-frequency and high-frequency modes in the vicinity of 3 T operational frequency. In order to estimate the coupling of the body birdcage coil to the modes of the dielectric resonators, we calculated the transmit efficiency [Fig. 3(b)]. The transmit efficiency was evaluated as the B_1^+-field value normalized to an accepted power of 1 W and averaged over the central cross section of the resonators. As a result, the $|B_1^+|$ values (mean values over the resonators) were 1.3 μT for the high-frequency mode and 0.6 μT for the low-frequency mode. For the reference case (when the birdcage coil is simulated without resonators), the mean $|B_1^+|$ value was 0.2 μT. As a result, the maximum transmit efficiency enhancement of a factor of 6.5 is achieved for the high-frequency mode (with symmetric field distribution) case in comparison with the reference one.

To study the performance of the proposed system experimentally, we fabricated the prototype [Fig. 4(a)]. Each dielectric resonator is made from four ceramic rings ($BaSrTiO_3$, including Mg-containing compositions[18]), which were serially placed on a thin supporting plastic tube. Each ring had the following dimensions: the inner diameter of 126.4 mm, the outer diameter of 149.2 mm, and the height of 27 mm. The relative permittivity of the ring material was $\varepsilon \sim 870$, and the dielectric loss tangent was 12×10^{-4} measured at 123 MHz (see the supplementary material for details).

Tuning of high-frequency mode (with symmetric field distribution) to 123 MHz (that corresponds to the proton Larmor frequency

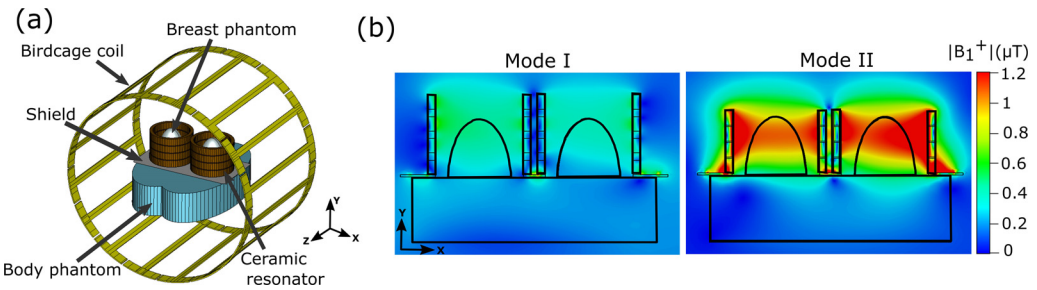

FIG. 3. (a) Setup of a numerical model with resonators placed inside body birdcage coil. (b) B_1^+-field distributions (root-mean-squared value) in the XY cross section normalized to the accepted power of 1 W. Both low-frequency (mode I) and high-frequency (mode II) modes were tuned to 123 MHz by slight modifications of the height of the resonators before placement inside the body birdcage coil.

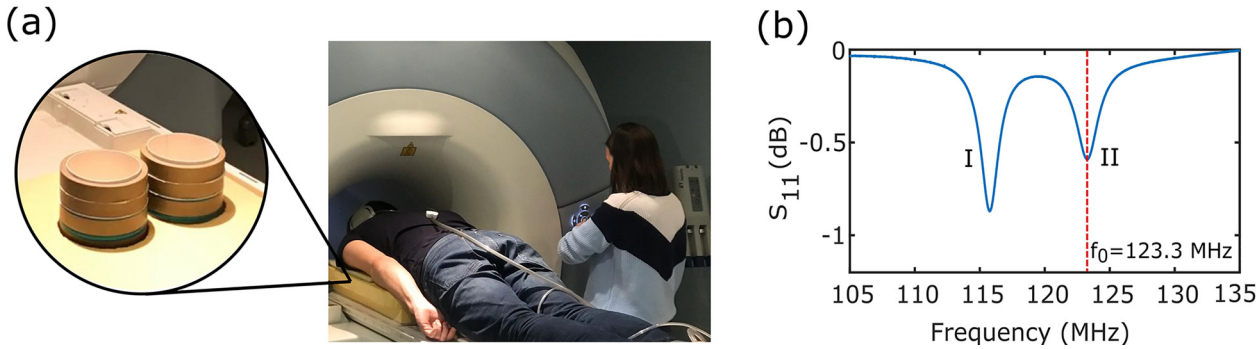

FIG. 4. (a) Photo of the prototype and MRI experiment. (b) The reflection coefficient (S_{11}) of the loop coil placed next to the resonators for a 16 cm distance between their centers. f_0 denotes the nuclear magnetic resonance frequency of protons at 3 T. The low-frequency (mode I) and high-frequency (mode II) modes are indicated.

at the given 3 T MRI scanner) was achieved by changing the spacing between the ceramic rings. Generally, spacers can be made from the low-permittivity and low-loss materials, like plexiglas, plastic, or thick paper. Here, we used several thin disks made of plexiglas with $\varepsilon \sim 3.5$ and $\sigma \sim 0.02$ S/m with heights of 1.5 and 3 mm, and several disks made of paper with $\varepsilon \sim 2.3$ with the height of 0.25 mm. All spacers had the inner and outer diameters as ceramic disks and were placed in the same support tube between the ceramic rings. The metallic plate used to preserve the efficiency of the dielectric resonator in proximity to the chest was made of the 14 μm-thick aluminum foil. The metallic plate was sufficiently thin to avoid distortion of the gradient magnetic fields necessary for spatial encoding of the MR signal. The aluminum foil was fixed on a rectangular plexiglas plate (with dimensions of 390×220 mm^2 and 2 mm thick) with two round holes (with a diameter equal to the outer diameter of the ceramic rings). The plexiglas plate with foil covering was fixed on the upper surface of the case so that there was no gap between it and top ceramic rings. As was mentioned above, the distance between the centers of the resonators was $d = 16$ cm since this distance is considered to be anatomically suitable for most women. Finally, the prototype was placed inside an extruded polystyrene case with two cylindrical holes to fix the resonators and provide the proper location of the breast phantoms inside the ceramic resonators during the MR study [Fig. 4(a)].

MR experiments were performed on a 3 T Siemens Magnetom Verio whole-body clinical system. Phantoms with dimensions and shapes appropriate to imitate breasts were placed inside the resonators, and the male body lay on the polystyrene case at the prone position to provide an appropriate load [Fig. 4(a)]. The high-frequency mode (with symmetric field distribution) was tuned to 123 MHz using a small loop antenna placed next to one of the resonators. Figure 4(b) shows the reflection coefficient (S_{11}) of the loop, where two minima were distinguished. The first minimum corresponds to the low-frequency mode (mode I) and the second minimum—to the high-frequency (mode II), which was tuned precisely to the operational frequency of 3 T. Two setups depicted in Fig. 5(a) were studied. The first configuration was the body birdcage coil used in transmitting mode with the multi-channel spine coil (two segments) used in receive mode. The second configuration was the body birdcage coil used in both transmit and receive modes in the presence of the resonators.

The placement of the subwavelength resonator within the body birdcage coil resulted in two effects. The first one is the improvement of transmit efficiency due to the focusing of the radio frequency magnetic field in the region of interest. As a consequence, this leads to the reduction of applied radiofrequency power.[23] The second effect is a substantial improvement of the birdcage local receive sensitivity within the area of the resonator.[24] Both effects are observed with a described system. The placement of the resonator allows us to reduce applied voltage amplitude required to create a certain B_1^+ field amplitude (see the supplementary material for details) 7.9 times in comparison with the case without dielectric resonators, thus making an entire examination safer. To estimate the influence of dielectric resonators on the receive sensitivity of the birdcage coil, we acquired the phantom

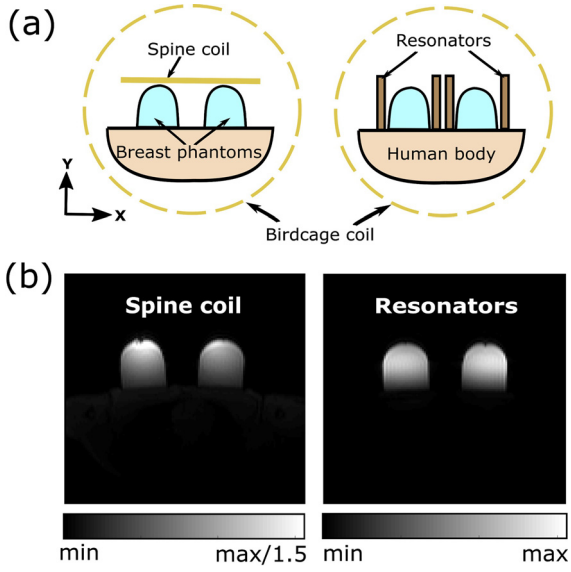

FIG. 5. (a) MRI experimental setup. The left panel shows the configuration with the body birdcage coil used in transmitting mode and the multi-channel spine coil used in receive mode. The right panel shows the body birdcage coil used in both transmit and receive modes in the presence of the resonators. (b) MR images of the phantom for the reference case (spine coil) and the proposed system of two dielectric resonators tuned to the symmetric mode. Phantom images were acquired using a gradient echo sequence: field of view 500×500 mm^2; acquisition matrix 128×128; slice thickness 3 mm; repetition time (TR) 500 ms; echo time (TE) 2.31 ms; flip angle 10°.

images. Figure 5(b) shows obtained MR images for both setups. SNR in MRI is one of the most crucial parameters that affect the quality of the MR image (see the supplementary material for details). To evaluate the SNR value, we divided the mean value of the signal in the area of the phantoms by the standard deviation of the noise, which was measured separately for zero input voltage. The SNR increase averaged over the region of interest was 1.5 times higher with the proposed system in comparison with the reference case.

In conclusion, we have proposed the system of coupled dielectric resonators composed of Mg-doped $BaSrTiO_3$ with a relative permittivity of $\varepsilon \sim 870$ and a dielectric loss tangent of 12×10^{-4} at 123 MHz for bilateral breast imaging. We analyzed the coupling between two dielectric resonators and demonstrated the impact of different mode excitation on the sensitivity of the MRI machine. Moreover, we experimentally observed that the coupling of symmetric-like mode to the radiofrequency birdcage coil gives rise to the improvement of both RF safety and sensitivity. The proposed structure can be directly employed in clinical MRI for application in bilateral breast imaging, including breast cancer screening.[25,26] Further improvements in the design of the resonator can be achieved via novel mechanisms for achieving high Q-factors[27] and with the excitation of non-radiative anapole states.[28,29] The results presented in this paper provide a possibility to develop very efficient devices based on dielectric resonators for substantial enhancement of MRI sensitivity.

See the supplementary material for a complete description of the dielectric loss tangent measurements, signal-to-noise ratio calculations, and numerical results relater to plane wave excitations and to the estimation of transmit efficiency.

The numerical calculations with the birdcage coil and experimental studies were supported by the Russian Science Foundation (Grant No. 18-75-10088). The numerical studies with the plane wave excitations were supported by the Russian Foundation for Basic Research (Grant No. 18-32-20115).

DATA AVAILABILITY

The data that support the findings of this study are available from the corresponding author upon reasonable request.

REFERENCES

[1]D. Kajfez and P. Gullion, *Dielectric Resonators* (Noble Publishing Corporation, Atlanta, GA, 1998).
[2]R. K. Moniga and A. Ittipiboon, IEEE Trans. Antennas Propag. **45**, 1348 (1997).
[3]R. K. Mongia and P. Bhartia, J. Microw. Mill.–Wave Comput.–Aided Eng. **4**, 230–247 (1994).
[4]A. G. Webb, Concepts Magn. Reson. **38A**, 148 (2011).
[5]H. Wen, F. A. Jaffer, T. J. Denison, S. Duewell, A. S. Chesnick, and R. S. Balaban, J. Magn. Reson. B **110**, 117 (1996).
[6]Q. X. Yang, J. Wang, J. Wang, C. M. Collins, C. Wang, and M. B. Smith, Magn. Reson. Med. **65**, 358 (2011).
[7]W. M. Teeuwisse, W. M. Brink, K. N. Haines, and A. G. Webb, Magn. Reson. Med. **67**, 912 (2012).
[8]T. P. O'Reilly, T. Ruytenberg, and A. G. Webb, Magn. Reson. Med. **79**, 1781 (2018).
[9]S. A. Aussenhofer and A. G. Webb, Magn. Reson. Med. **68**, 1325 (2012).
[10]R. Schmidt, W. Teeuwisse, and A. Webb, Magn. Reson. Med. **77**, 2431 (2017).
[11]T. Ruytenberg and A. G. Webb, J. Magn. Reson. **284**, 94 (2017).
[12]T. Neuberger, V. Tyagi, E. Semouchkina, M. Lanagan, A. Baker, K. Haines, and A. G. Webb, Concepts Magn. Reson. **33B**, 109 (2008).
[13]K. Haines, T. Neuberger, M. Lanagan, E. Semouchkina, and A. G. Webb, J. Magn. Reson. **200**, 349 (2009).
[14]M. Moussu, L. Ciobanu, S. Kurdjumov, E. Nenasheva, B. Djemai, M. Dubois, A. G. Webb, S. Enoch, P. Belov, R. Abdeddaim, and S. Glybovski, Adv. Mater. **31**, 1900912 (2019).
[15]A. A. Mikhailovskaya, A. V. Shchelokova, D. A. Dobrykh, I. V. Sushkov, A. P. Slobozhanyuk, and A. Webb, J. Magn. Reson. **291**, 47 (2018).
[16]M. Song, P. Belov, and P. Kapitanova, Appl. Phys. Lett. **109**, 223902 (2016).
[17]I. Zivkovic, W. Teeuwisse, A. Slobozhanyuk, E. Nenasheva, and A. Webb, J. Magn. Reson. **299**, 59 (2019).
[18]E. A. Nenasheva, N. F. Kartenko, I. M. Gaidamaka, O. N. Trubitsyna, S. S. Redozubov, A. I. Dedyk, and A. D. Kanareykin, J. Eur. Ceram. Soc. **30**(2), 395–400 (2010).
[19]A. Shchelokova, V. Ivanov, A. Mikhailovskaya, E. Kretov, I. Sushkov, S. Serebryakova, E. Nenasheva, I. Melchakova, P. Belov, A. Slobozhanyuk, and A. Andreychenko, Nat. Commun. **11**, 3840 (2020).
[20]P. D. Friedman, S. V. Swaminathan, K. Herman, and L. Kalisher, Am. J. Roentgenol. **187**, 345–349 (2006).
[21]A. G. Webb, J. Magn. Reson. **216**, 107 (2012).
[22]E. Vandeweyer and D. Hertens, Ann. Anat. **184**(2), 181–184 (2002).
[23]A. V. Shchelokova, A. P. Slobozhanyuk, P. de Bruin, I. Zivkovic, E. Kallos, P. A. Belov, and A. Webb, J. Magn. Reson. **286**, 78 (2018).
[24]A. V. Shchelokova, A. P. Slobozhanyuk, I. V. Melchakova, S. B. Glybovski, A. G. Webb, Y. S. Kivshar, and P. A. Belov, Phys. Rev. Appl. **9**, 014020 (2018).
[25]S. E. Harms, Curr. Probl. Diagn. Radiol. **25**(6), 192–215 (1996).
[26]M. Morrow, J. Waters, and E. Morris, Lancet **378**, 1804 (2011).
[27]M. V. Rybin, K. L. Koshelev, Z. F. Sadrieva, K. B. Samusev, A. A. Bogdanov, M. F. Limonov, and Y. S. Kivshar, Phys. Rev. Lett. **119**, 243901 (2017).
[28]A. E. Miroshnichenko, A. B. Evlyukhin, Y. F. Yu, R. M. Bakker, A. Chipouline, A. I. Kuznetsov, B. Luk'yanchuk, B. N. Chichkov, and Y. S. Kivshar, Nat. Commun. **6**, 8069 (2015).
[29]K. Baryshnikova, D. Filonov, C. Simovski, A. Evlyukhin, A. Kadochkin, E. Nenasheva, P. Ginzburg, and A. S. Shalin, Phys. Rev. B **98**, 165419 (2018).